



A deep learning-based battery sizing optimization tool for hybridizing generation plants

March 2024

Changing the World's Energy Future

Yingqian Lin, Binghui Li, Vivek Kumar Singh, Thomas M Mosier, S M Shafiul Alam, Jonghwan Kwon, Sangwook Kim, Tanvir R Tanim, L. Michael Griffel, Hill Balliet, Matthew R. Mahalik



DISCLAIMER

This information was prepared as an account of work sponsored by an agency of the U.S. Government. Neither the U.S. Government nor any agency thereof, nor any of their employees, makes any warranty, expressed or implied, or assumes any legal liability or responsibility for the accuracy, completeness, or usefulness, of any information, apparatus, product, or process disclosed, or represents that its use would not infringe privately owned rights. References herein to any specific commercial product, process, or service by trade name, trade mark, manufacturer, or otherwise, does not necessarily constitute or imply its endorsement, recommendation, or favoring by the U.S. Government or any agency thereof. The views and opinions of authors expressed herein do not necessarily state or reflect those of the U.S. Government or any agency thereof.

A deep learning-based battery sizing optimization tool for hybridizing generation plants

**Yingqian Lin, Binghui Li, Vivek Kumar Singh, Thomas M Mosier, S M Shafiul
Alam, Jonghwan Kwon, Sangwook Kim, Tanvir R Tanim, L. Michael Griffel, Hill
Balliet, Matthew R. Mahalik**

March 2024

**Idaho National Laboratory
Idaho Falls, Idaho 83415**

<http://www.inl.gov>

**Prepared for the
U.S. Department of Energy
Under DOE Idaho Operations Office
Contract DE-AC07-05ID14517**

A Deep Learning-based Battery Sizing Optimization Tool for Hybridizing Generation Plants

Yingqian Lin¹, Binghui Li¹, Vivek Kumar Singh¹, Thomas M. Mosier¹, Sangwook Kim¹, Tanvir R. Tanim¹, L. Michael Griffel¹, S. M. Shafiul Alam¹, Hill Balliet¹, Matthew R. Mahalik², Jonghwan Kwon²

¹Idaho National Laboratory, Idaho Fall, ID

²Argonne National Laboratory, Lemont, IL

Keywords: Renewable energy; Energy storage; Hydropower; Deep learning; Battery sizing optimization.

Abstract

Hybrid generation and energy storage systems can enhance asset flexibility, enabling various services and optimizing financial performance. From a generation asset owner perspective, the decision to hybridize includes selecting an energy storage system that maximizes financial performance of the energy storage investment. Yet, existing tools to optimize energy storage sizing are either too rudimentary or too complex for most asset owners to implement (i.e., require specialized engineering and software knowledge and a high-performance computer to run).

This work presents a deep learning-based battery sizing optimization tool for hybridizing generation facilities. The tool uses deep learning technique to predict revenue over a broad search space of potential battery sizes, estimate capital and operations costs (including accounting for battery degradation), and calculate financial performance of each potential battery system investment; an output is a recommendation of battery that maximizes financial performance. The tool is tested and validated for hydropower generation and is publicly available on Idaho National Laboratory's GitHub page (https://github.com/idaholab/Hydro_Hybrids), documented in Zenodo (<https://zenodo.org/record/7562692#.Y9Q7anbMKUm>), and accessible through an intuitive web app (hydrohybrids.inl.gov). This tool will help a greater cross-section of generation owners consider investments in battery systems, increasing their revenue and helping them compete in rapidly evolving

electrify markets.

Nomenclature	
Symbol	Description
	Energy rating of a battery (MWh)
	Power capacity of a battery (MW)
	Energy rating of battery normalized by paired plant capacity (MWh/MW)
	Power rating of battery normalized by paired plant capacity (dimensionless)
	Minimum charge (%)
	Maximum charge (%)
	Total round-trip efficiency (%)
	Energy prices (\$/MWh)
	Regulation up prices (\$/MWh)
	Regulation down prices (\$/MWh)
	Spinning service prices (\$/MWh)
	Non-spinning service prices (\$/MWh)
	Energy from energy storage device to grid (MWh)
	Energy from energy storage device to regulation up service (MWh)
	Energy from energy storage device to regulation down service (MWh)
	Energy from energy storage device to spinning service (MWh)
	Capacity loss/fade of energy storage in Ah
	Capacity loss/fade of energy storage in %
	Generated hydropower that is available to battery (MW)
	Generated hydropower that is available to battery and normalized by maximum plant capacity (dimensionless)
	Battery construction and commission cost (\$/kWh)
	Battery capital and management systems cost (\$/kWh)
	Capital cost of power conversion system (\$/kW)
	Capital cost of balance of plant (\$/kW)
	Fixed operations and maintenance cost (\$/kW-yr)
	Depreciation rate (%)
	Discount rate for NPV (%): 10-yr treasury bonds
	Federal and state income tax rate (%)
	Battery life span (years)
	Life span for other equipment such as power conversion system (years)

1. Introduction

1.1. Importance of hybridization for enhancing financial performance

There is increasing interest in hybridization of generation and storage assets based on the resulting higher business value compared to investing in the standalone assets. It has been found that wholesale electricity market net revenue is higher for generation plus storage hybrids compared to standalone generation projects [1]. Hybridization of energy storage with a renewable generation asset also increases net value irrespective of the changes in generator operations [2]. Furthermore, increasing penetration of non-dispatchable renewable energy resources impacts the time of pricing and hence has historically decreased market value of baseload generation, increasing motivation for hybridization with energy storage [3].

Generation and storage asset hybridization adds operational flexibility. For a non-dispatchable generation resource, this flexibility can help avoid the penalty of not meeting dispatch commitment and reducing generation curtailment [4]. The flexibility also increases energy arbitrage potential and supports load shifting, resulting in additional net revenue due to electricity market temporal variations in prices at a given location [5]. Hybridization can also complement ramping constraints of generation assets and hence improve response or add new participation to the ancillary service markets [6]. Complementing generation asset's ramping constraints can also reduce operation and maintenance costs [7-9]. Hill, et al. [10] has reported that a photovoltaics-coupled battery energy storage system reduced the system ramp rate from 4 MW/min (solar standalone) to less than 50 kW/min, which significantly reduced in wear and tear of the diesel generators. Hybridization can also improve resilience through enabling black start and hence reduce costs of outages [11].

For the current application, this tool has been trained and developed for run-of-river (ROR) hydropower hybridization. Training the model to a specific generation technology allows it to account for generation specific value propositions, but it means that the applicability of this tool is sensitive to how well the end user's scenario matches the training data. For example, hybridizing ROR hydropower can

reduce variability and improve capacity value, but the value of doing this is different from solar and wind because of the difference in generation profile and predictability. For reservoir hydropower plants, hybridization can reduce the cost of environmental compliance and operations and maintenance. In fact, new modes of operation and increased flexibility can lead to improved environmental performance and increased revenue at the same time [12].

1.2. Battery degradation cost

Representing battery degradation in hybridization modeling is important to account for real performance characteristics over the lifetime of the hybrid asset. Substantial efforts have been made to develop battery degradation models and have confirmed that it is a complex nonlinear process dependent on several factors such as temperature, charging/discharging current intensity, depth of discharge [13-15]. The effects of battery degradation in terms of technical performance can be categorized into capacity fade and resistance growth, which respectively lead to a reduction in the energy and power capacities. Capacity fade is primarily caused by the loss of cyclable lithium ions, whereas power fade is largely caused by the increase in cell impedance.

Battery degradation factors are often binned as “cycle aging” and “calendar aging”, both of which are considered in this work. Parasitic reactions between electrolyte and electrode (e.g., solid electrolyte interphase (SEI) growth, electrolyte oxidation, and transition metal dissolution) are assumed to be dominant mechanism for both cycling and calendar aging [16]. Calendar aging refers to the aging process of a battery even when it is not in use. The reaction rate during calendaring aging is mainly affected by ambient temperature and state of charge (SOC). By contrast, cycle aging represents the aging mechanism based on battery use. The rate during cycling depends on charging/discharging current, depth of discharge, cycle numbers, and cut-off voltage in addition to the factors affecting calendaring aging [17].

1.3. Knowledge gaps and motivation

Research on the hybridization of generation assets with energy storage systems mostly focuses on the sizing (in terms of power capacity, storage duration) and siting (geographic proximity, electrical co-

location, placement behind the interconnection, etc.) of energy storage systems, control strategies of the asset mix (e.g., independent, coordinated, hierarchical, etc.) [18], and challenges in hybrid system design optimization and economic performance evaluation still exist [10].

Most existing tools with the capability to select energy storage systems for pairing with generation assets require extensive expertise to run. For example, the Revenue Operation and Device Optimization (RODeO) and the Conventional Hydropower Energy and Environmental Systems (CHEERS) models are unit commit and economic dispatch tools that can be configured to optimize market participation of hybrid generation and energy storage systems [19, 20]. To implement these models, a user must be familiar with the programming language, respectively GAMS and LINDO, and must implement a separate simulation for each change in market conditions, generation, or energy storage configuration. Each run takes on average several hours to complete, so optimization of the generation and energy storage hybrid may take several days of just computational time, the results of which must also be analyzed by an expert. This is prohibitive to many potential users. Based on this barrier, consultants often use oversimplified analyses based on rules of thumb or that do not precisely account for factors such as market dynamics.

There are some emerging tools to evaluate energy storage as a standalone asset. For example, the Battery Energy Storage Evaluation Tool that is developed by the Pacific Northwest National Laboratory lets users identify the services that a battery would provide and then can evaluate financial performance of a battery system, including exploring over a search space [21]. The Renewable Energy Integration and Optimization and the System Advisor Model developed by the National Renewable Energy Laboratory also let users perform energy storage technoeconomic assessment [22, 23]. These models are all important contributions to the overall wealth of knowledge aiding energy storage decision making, but a few gaps remain including (a) these tools are principally focused on standalone energy storage systems, (b) they don't account for battery degradation, which is an important driver of cost and performance, and (c) most of the developed tools require user knowledge of the programming language and are computationally expensive to implement.

1.4. Battery sizing optimization tool for generation and battery hybrid

This paper presents the development, validation and application of a battery sizing optimization tool, which is designed to help generation asset owners efficiently take the first step of considering energy storage devices based on maximizing financial performance of the hybrid asset. The model assumes that the generation asset is already optimized and requires market conditions as an input for performing the battery sizing optimization. The tool is principally designed for generation assets participating in competitive electricity markets, e.g., the California Independent System Operator (CAISO), Electric Reliability Council of Texas (ERCOT), and the PJM Interconnection, where there is an explicit set of market products and corresponding time-varying prices. The tool is applicable to all forms of generators that are either variable renewable resources (e.g., wind, solar, tidal, and run-of-river hydropower) or dispatchable but slow ramping (i.e., hydropower with reservoir or nuclear). For generation assets with flexibility, e.g., a hydropower plant with reservoir, the model assumes that the generation plant's dispatch is already optimized and therefore the tool treats the generation profile as fixed (i.e., it only shapes the battery usage profile).

The sizing tool uses machine learning (ML) models that are trained on a broad set of dispatch simulations to predict revenue and cycling of the hybrid generation and battery asset (Figure 1 – left section). These dispatch simulations are used to train ML models to predict revenue and battery degradation. These ML predictions are combined with battery capital and operation cost calculation to assess multi-year technoeconomic performance of the battery investment hybridized with an existing generation asset.

When the user is implementing the model, the user-supplied inputs are simply generation and market price profiles (Figure 1 – top right section). Based on these user-supplied inputs, the tool searches a plausible set of battery sizes (power and duration) and selects the size with the best financial performance, as determined by the metric of interest to the user. Example metrics are return on investment (ROI), payback period, or net present value over 10-year period given specific discount rate. The tool also provides the financial performance for other battery sizes in case the user is interested in alternative sizes

that result in inferior financial performance to meet other constraints (e.g., interconnection limit or battery system purchase price).

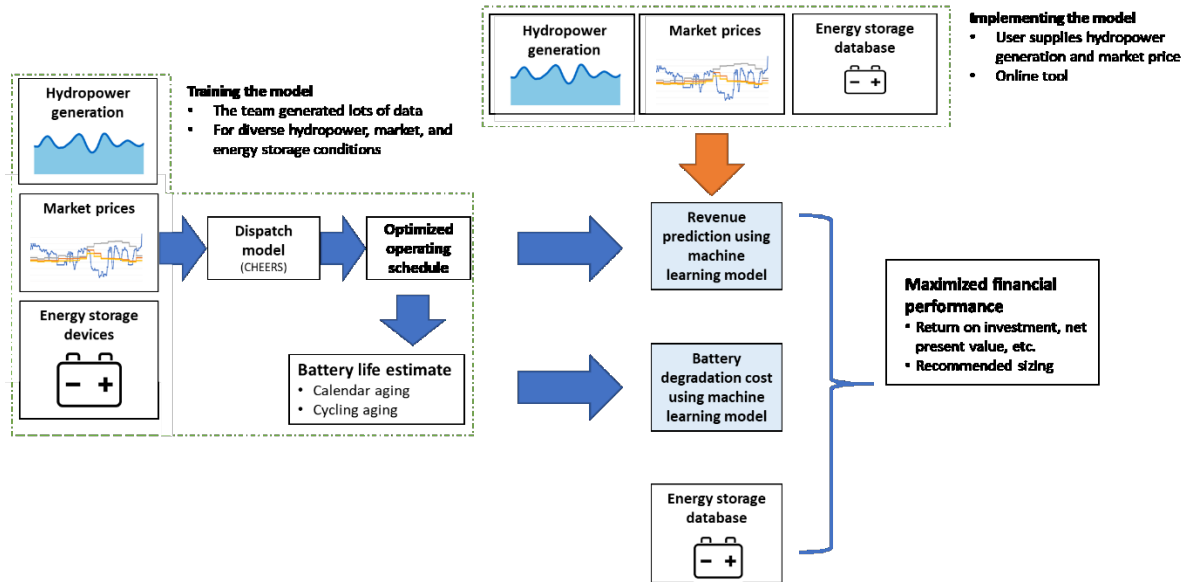


Figure 1. Conceptual data flow in the developed financial performances optimization tool. The blue arrows indicate data flow related with training and testing of the ML model, and the orange arrow indicates data flow related with model implementation.

1.5. Machine learning in renewable energy optimization

In the recent literatures, ML applications have emerged as pivotal in advancing the renewable energy sector, particularly in predictive analytics and operation optimization. [24] unveiled the significant impact of green technology innovation on energy transitions in China, utilizing ML methods to decipher the relationship between financial support and the energy transition procedure. Similarly, [25] employed ML in predicting rural power outages in Iran, illustrating a valuable framework where hybrid renewable energy systems can be economically and effectively deployed to alleviate predicted outages. Furthermore, [26] et al. underscored the imperative synergy between ML and optimization techniques in integrated energy systems, revealing a critical research gap in leveraging these technologies for improved IES planning and sustainability. Diving into operation rules and their implications, [27] utilized a deep learning model with an attention mechanism to extract operational rules in wind-solar-hydro hybrid systems amidst multifaceted uncertainties, showcasing improved decision-making efficacy. Similarly,

another study by [28] introduced a novel CNN-FEM framework for the cost-efficient analysis of fluid–structure interaction in hydrofoil, paving the way for efficient and optimized design in tidal turbines with morphing blades. Collectively, these papers illuminate the current trajectory where ML and deep learning models stand central to enhancing predictability, decision-making, and operational efficiency in various domains of the renewable energy sector, offering a rich tapestry of insights and methodologies that could shape future research and applications in sustainable energy.

The key contributions and novelties of this study are:

- Existing tools to optimize energy storage sizing are either too rudimentary (i.e., based on “rules of thumb”) or too complex for most asset owners to implement (i.e., require specialized engineering and software knowledge and a high-performance computer to run). The developed ML-based tool provides a new approach to do sizing optimization for a hydropower plant to integrate battery storage system based on different financial performance metrics.
- In previous studies, battery degradation or depreciation costs were primarily associated with calendar aging. However, this study is among the first to assess the financial performance of batteries by considering both calendar aging and cycle aging.
- Compared to existing tools, this developed model only requires simple user-supplied inputs (generation and market price profiles) to provide fast and straight-forward battery sizing and financial performance optimization for hybrid energy generation and storage system.

The remainder of this paper is organized as follows. Section 2 provides a detailed description of the methodologies used in this paper, including the market participation optimization tool (CHEERS) that provides the training data to the ML model, the battery degradation modeling, the ML techniques utilized, and the financial performance evaluation metrics considered in this tool. Section 3 presents the validation results for revenue and battery degradation cost prediction by using the developed ML models, and battery sizing optimization in various scenarios, model limitations, and potential future work directions. Section 4 presents key conclusions from this study.

2. Methods

The main elements of the tool are revenue prediction, battery degradation prediction, battery system cost estimation, and financial performance evaluation. The last of these four elements is used to recommend a battery size for hybridizing with a specific generation asset. This section is organized to describe (1) the daily revenue optimization model, (2) the battery degradation model, (3) the machine learning models used in revenue and battery degradation prediction (including training and test data, and evaluation of the ML models), and (4) the battery system cost and financial performance evaluation.

2.1. The modeled system

Our modeled hydro hybrid system (Figure 2) includes a run-of-river hydropower plant and a utility-scale battery storage system and receives revenue by selling electricity to a real-time electricity market. We consider both energy and ancillary markets, the latter of which includes regulation-up, regulation-down, spinning reserve, and non-spinning reserve. We assume the battery can only charge from the hydropower plant (i.e., it is not allowed to charge from the grid). We maximize total revenue by optimizing operations of the hybrid system, such as electricity charged to and discharged from the battery, electricity sold to the energy market, and provision of all ancillary services.

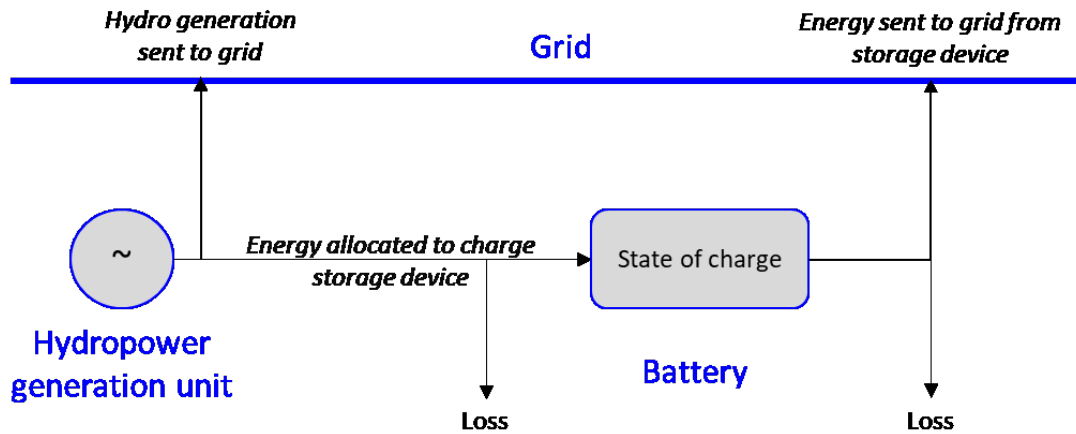


Figure 2. The modeled hydro hybrid system with electricity input and output flow. We assume that the electricity to the battery can only be provided by the hydropower unit.

Our model is constructed as a MILP problem and solved by CHEERS. The CHEERS model is developed by the Argonne National Laboratory and is a component of the Water Use Optimization

Toolset (WUOT), which itself is developed to provide dispatch guidance for hydropower operators [29]. Users of the model can create a node-and-link-based network representation of the optimized system and enter equations and constraints to describe the objectives and limitations of the system and its individual components. CHEERS converts user inputs to a MILP problem which is then solved by LINGO [30]. CHEERS can be used for many different types of networks and mass and/or energy flow problems that extend beyond hydropower and power system applications.

The inputs to the CHEERS model are hydropower generation profiles (5-minute timeseries), market price profiles of the considered energy and ancillary service products (5-minute timeseries), and techno-economic parameters of the modeled hydro hybrid system, such as hydropower plant capacity, power and energy ratings of the battery, round-trip efficiency, and maximum charge/discharge rates. Each model run corresponds to one year of conditions. CHEERS optimizes each day independently by assuming equal state of charge at the beginning and end of the day. In this work, we use historical water flow rate [31] to calculate the hydropower generation profiles by assuming that electricity generated from the hydropower plant is solely determined by incoming water flow. The test cases also use real-time CAISO 2018 and 2019 energy and ancillary service market prices.

Our study examines five hydropower plants, the rated capacities of which range from 1.42 MW to 30 MW (Table 1). Because of the wide range of hydropower capacities, the batteries paired to a hydropower plant are rated at the 20th and 80th percentiles of each plant's power duration curve. We consider three storage durations of 0.5, 2, and 4 hours for each battery power rating because these durations represent the most common utility-scale battery storage durations in the U.S [32]. Each hydropower plant is therefore paired with six different battery configurations during the CHEERS training simulations, resulting in 36 hydro hybrid system configurations used in ML model training. The detailed technical parameters of all 36 systems are tabulated in Table S1.

Table 1. Hydropower plant characteristics and market price profiles used in this study.

Plant	A	B	C	D	E	F¹
State	California	Pennsylvania	California	Ohio	Michigan	Ohio
Plant characteristics Capacity (MW)	3.1	30.0	13.4	2.2	1.42	2.2
Annual generation (MWh)	2,936	37,185	60,705	11,152	10,695	15,582
Capacity Factor (CF)	0.11	0.36	0.52	0.58	0.96	0.81
Market prices Source	CAISO					
Node	GOLDHILL_1_N033					

Notes:

1. F's energy profile is scaled up by a factor of 3.5 from plant D's 2012 energy profile.

2.2. Battery degradation modeling

This analysis uses the anode SEI aging model coupled with the nonlinear, electrolyte-enhanced, single particle model (NESPM) [33] to characterize the capacity fade of lithium-ion batteries. The model has been successfully implemented for developing battery life enhancing management and control strategies [34, 35]. In this model, it is assumed that SEI growth in anode is a main aging mechanism during both calendaring and cycling aging. [33] represents the capacity fade of a lithium-ion battery under repetitive cycles as

where F ($C \cdot mol^{-1}$) is the Faraday constant, R ($J \cdot K^{-1} \cdot mol^{-1}$) is the gas constant, T (K) is temperature, A ($A \cdot cm^{-2}$) represents side reaction exchange current density, and S (cm^2) and L (cm) represent the area and thickness of negative electrolyte, respectively. τ (s) represents cycle period and V (V) represents the average SEI overpotential. Both A and S are a function of the average SOC. I_{RMS} (A) is the root mean square (RMS) current over a cycle. By including cycle time, τ , and mean SOC this model accounts for calendar aging when $\tau \gg t_{cycle}$, which accounts for cycle aging in both charging and discharging processes. The parameters A , S , and L , representing SEI growth rates, were carefully adjusted to align with empirical data derived from previous studies [33, 34]. Specifically, we tuned the A parameters for calendar and cycling aging to 3.1×10^{-13}

A/cm² and 1.24×10^{-12} A/cm², respectively, to ensure that our model reproduces the observed behaviors in both aging scenarios. The performance of cells and aging parameters in this model are validated with commercial graphite/LFP cells where batteries undergo identical charge/discharge cycles [36]. Note that temperature is assumed to be held constant at 298.15 K (25 °C). In future studies, we will consider the impact of temperature on battery degradation.

We apply the degradation model in Eq. (1) to all model runs to calculate daily capacity fade and sum up the daily values to obtain annual capacity fade. In addition, we consider three capacity fade rates (i.e., the low, medium, and high scenarios) to account for uncertainties associated with battery life performances, as shown in Table 2. These scenarios are distinguished by different aging parameters, tuned to reflect the desired capacity fade rates. Note that these scenarios are selected based on capacity retention of commercial cylindrical batteries under various degradation conditions [37] to encompass a wide range of battery performances from multiple manufacturers. The results indicate that longer storage durations typically lead to less capacity fade when other factors are held constant. For example, when the storage hour increases from 0.5 hour to 4 hours, the capacity fade reduces from 2.7% in Run #6 to 2.1% in Run #2 in the Low scenario. In addition, when everything else is kept constant, increasing the power capacity tends to reduce the capacity fade. This is reflected by the drop of capacity fade from 2.8% in Run #1 to 2.1% in Run #2, when the power capacity is increased from 0.03 MW to 0.53 MW.

The primary reason that increasing storage duration reduces capacity fade is that the larger energy capacity leads to reduced cycling. When other parameters are held constant, increasing the storage duration results in a greater energy capacity, which further results in a reduced number of cycles when the same amount of energy is flowing through the battery. Since the number of cycles and capacity fade are positively correlated, an increase of storage duration will result in less capacity fade. Similar to increasing storage duration, increasing power capacity also results in a greater energy capacity and a corresponding lower capacity fade. In addition, when the same amount of power flows through a battery, the battery with a greater energy capacity has a smaller C-rate (i.e., smaller current in each cell). As Eq. (1) implies, a smaller RMS current results in less cycle aging.

Table 2. A summary of battery parameters and annual capacity fades from all model runs under different degradation rates. Note that the other parameters of each run can be found in Table S1.

Run	Power (MW)	Duration (h)	Loss (%)			Run	Power (MW)	Duration (h)	Loss (%)		
			Low	Mid	High				Low	Mid	High
1	0.03	4	2.8	7.6	15.32	19	0.24	4	3.1	8.7	17.51
2	0.53	4	2.1	5.0	9.71	20	1.55	4	2.4	6.0	11.67
3	0.03	2	2.8	7.5	15.02	21	0.24	2	3	8.2	16.63
4	0.53	2	2.4	5.8	11.43	22	1.55	2	2.5	6.2	12.19
5	0.03	0.5	2.9	8.0	16.03	23	0.24	0.5	3	8.1	16.30
6	0.53	0.5	2.7	6.9	13.79	24	1.55	0.5	2.9	7.7	15.52
7	3.3	4	2.2	5.2	10.06	25	0.85	4	3.1	8.7	17.55
8	10.8	4	1.8	3.8	6.91	26	1.24	4	3.1	8.5	17.08
9	3.3	2	2.1	5.0	9.61	27	0.85	2	3	8.2	16.57
10	10.8	2	1.9	4.3	8.17	28	1.24	2	3	8.2	16.63
11	3.3	0.5	2.3	5.5	10.63	29	0.85	0.5	3	8.2	16.42
12	10.8	0.5	2.2	5.3	10.21	30	1.24	0.5	3	8.3	16.62
13	3.22	4	3.1	8.5	17.20	31	0.96	4	3.1	8.5	17.20
14	7.91	4	2.4	6.2	12.17	32	1.7	4	2.9	8.0	16.08
15	3.22	2	2.9	8.0	16.14	33	0.96	2	2.9	8.0	16.12
16	7.91	2	2.8	7.6	15.33	34	1.7	2	3	8.1	16.23
17	3.22	0.5	2.9	7.9	15.88	35	0.96	0.5	2.9	7.9	15.83
18	7.91	0.5	3	8.1	16.28	36	1.7	0.5	2.9	7.9	15.91

Battery degradation cost is calculated as the additional cost required to replenish the capacity lost to degradation such that the system capacity remains constant throughout its lifetime [38]. The primary unit of estimated capacity fade, (Ah/yr), is over each year. The corresponding annual degradation cost is calculated as

where (Ah) is rated battery capacity, (\$/kWh) is the battery capital cost and (\$/yr) is the annual degradation cost. The ML model is then trained to predict annual degradation based on the daily calculations of cycling and associated capacity fading (see ML description in Section 2.3).

2.3. Machine learning models

2.3.1. Data for ML model training and test

Training and test data for the prediction module are produced using the CHEERS model, which optimizes 5-min unit dispatch to maximize daily market revenue of all 36 hydro hybrid systems [20]. Table 1 shows the six hydropower plants grouped based on their CF as “low CF,” “medium CF,” and

“high CF,” where each group includes two plants. We split the 36 CHEERS runs into two equally sized training and test sets, each of which includes a hydropower plant in each CF bin. Table S1 in the supplementary information lists the runs included in the training and test sets. Note that we use the same training and test sets as in our previous study [20].

2.3.2. Revenue prediction and results post-processing.

The revenue prediction ML model is an artificial neural network (ANN) with an 8-hr moving window configured as a densely connected multi-layer perceptron (MLP) [20]. Following the input layer, a series of hidden layers containing 64, 128, 256, 128, 64, 32, 16 nodes respectively are arranged in a sequential structure (Figure 3a). Each hidden layer is configured with a rectified linear unit (ReLU) activation function ([39]):

where σ is always positive and x , the neuron input, is not bounded in the positive direction. This activation function is commonly used as it converges faster, does not plateau or saturate in the positive direction, and it is sparsely activated as all negative inputs are converted to zero within the network.

The final output layer consists of five output nodes for each revenue prediction component. These daily revenue predictions are then aggregated to annual values, reflecting the associated diversity of conditions experienced both with respect to generation output and market conditions. A more detailed description of this model is given in [40].

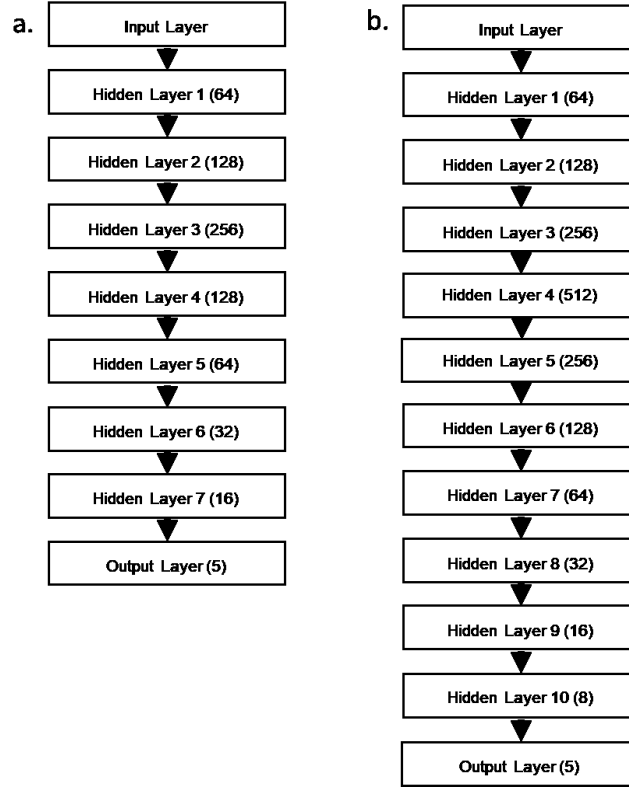


Figure 3. Model architecture for (a) the revenue prediction model and (b) the degradation prediction model.

To correct for negative or unrealistically high predicted daily revenues, a post-processing step is added to the ML model to impose lower and upper bounds on the predicted values. The lower bound of the total predicted revenue is set as the hydro energy only revenue as we assume that the total revenue from the optimization of the combined assets should be higher than the case without any energy storage. The upper bound of predicted revenue from each market is limited based on physical constraints appropriate to each revenue source. The equations used for applying the upper and lower bound are presented in [40].

2.3.3. Battery degradation prediction

Charging and discharging current profiles of a battery over the entire year must be given to apply the physics-based degradation model in (1), and this remains unknown until a dispatch optimization run is completed. We therefore resort to data-driven methods to enable fast degradation estimation to avoid time-consuming optimization runs. Similar to the revenue prediction model, we develop an ANN to

predict daily battery degradation. The main idea of the battery degradation prediction is to create a mapping between the profiles of battery degradation and the input at the training stage:

where X represents input features, Y represents output features, θ represents trainable ANN parameters, and f represents the mapping relationship between the input and output features. Thirteen input features are used to train the battery degradation ML model, which are selected based on correlation analysis conducted in [40]:

These are used to predict five features to calculate battery degradation:

The resulting degradation prediction model architecture has a series of 10 hidden layers containing 64, 128, 256, 512, 256, 128, 64, 32, 16, and 8 nodes arranged in a sequential structure (Figure 4b). Each hidden layer is configured with a rectified linear unit (ReLU) activation function and the models are optimized with the Adam function using a learning rate of 0.0001. The batch size or number of instances processed before the model is updated. During model training, we monitor mean absolute error (MAE) and apply the early stopping strategy, which stored the best model when the model stopped improving (or when the model loss/MAE stopped decreasing). At this point, we think the model has “adequately” learned the training data. [40]. The validation split ratio is 10% across all models. The trained ML degradation models adequately represent the pattern from the training data as the loss function of both the training and validation cases decrease through epochs (Figure 4). In addition, the learning curves show no over fitting issues, because validation errors are consistently greater than training errors.

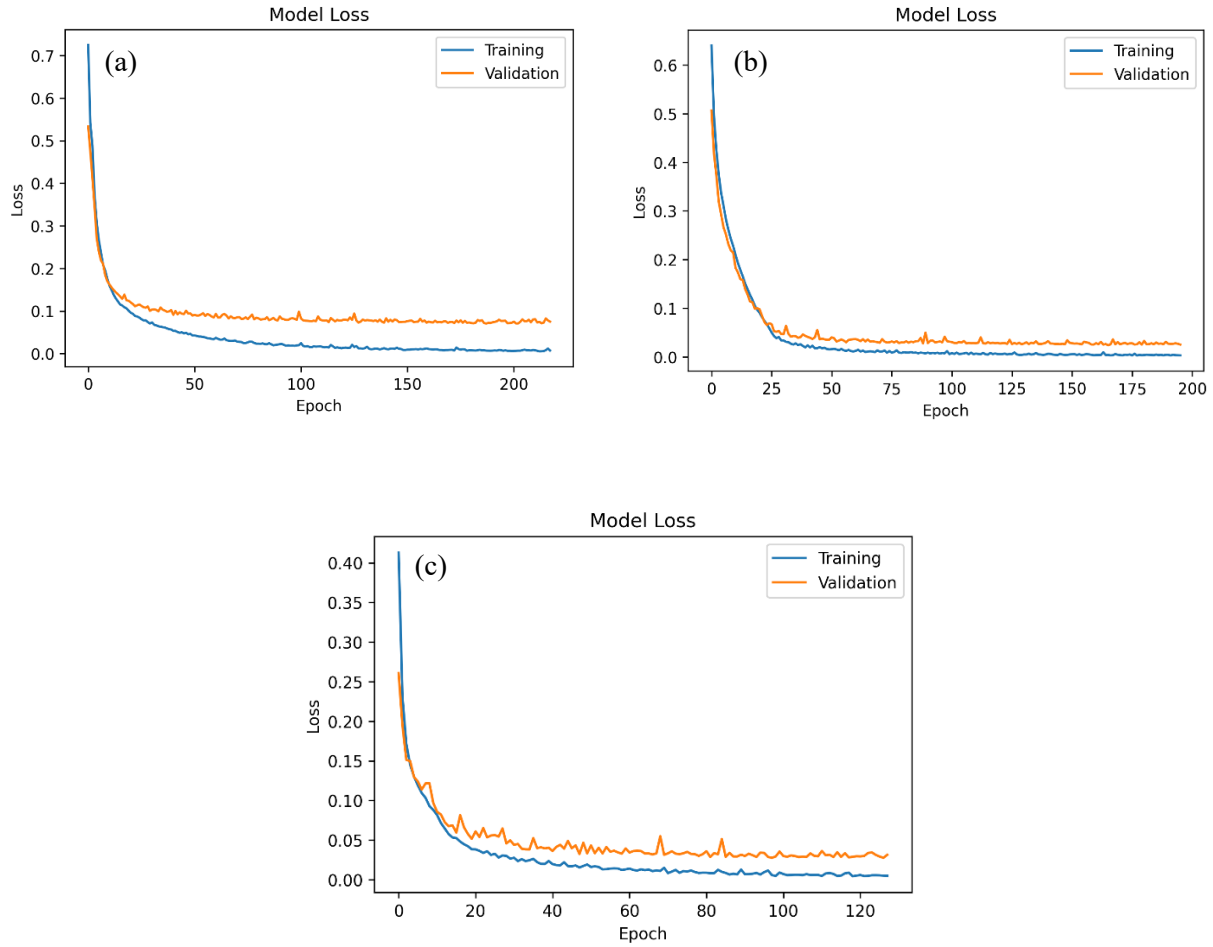


Figure 4. Learning curves for the battery degradation prediction models: (a) the low degradation rate scenario, (b) the medium degradation rate scenario, and (c) the high degradation rate scenario.

2.3.4. Evaluation metrics

Two metrics are used to evaluate the performance of both prediction models (Table 3): prediction percent error and the Root Mean Square Error (RMSE). Note that the percent error is computed to evaluate both annual and daily prediction accuracy, while the RMSE is calculated separately for each day and then averaged across days within a specified date range to evaluate daily prediction accuracy over a specific period. In Table 3, N denotes the total number of days in the evaluated period, and \hat{y}_t and y_t represent the actual and predicted value on the t day, respectively. For example, when calculating percent error (Eq. (4)), \hat{y}_t for daily percent error and \bar{y} for annual percent error.

Table 3. Evaluation metrics used in this study.

Metric	Equation
Percent error	(4)
RMSE	(5)

2.4. Financial performance evaluation

2.4.1. Cost and financial performance calculation

Techno-economic parameters used in financial performance evaluation, such as capital and operations costs, are drawn from [41] (Table 4), which estimates 2018 and projected 2025 costs for a broad range of [41] energy storage technologies. Based on the reported cost ranges, we consider six cost scenarios to account for parametric uncertainties, including 2018 low-, mid- and high- and 2025 low-, mid- and high-cost scenarios. The formulas used to calculate cost estimates for a given battery system are:

(6)

(7)

(8)

(9)

where Eq. (6) calculates the upfront capital investment of a battery storage system with a power rating of and energy rating of , Eq. (7) calculates annual operations and maintenance cost, Eq. (8) calculates annual depreciation cost of the battery pack, assuming linear depreciation over its lifetime, and Eq. (9) calculates depreciation cost of the balance of plant in the battery storage system.

Battery degradation cost is calculated as the additional cost required to counteract the degradation such that the system capacity remains constant throughout its lifetime [38]. The primary unit of estimated

capacity fade, (Ah/yr), is over each year. The ML model is used to predict annual degradation based on the daily calculations of cycling and associated capacity fading (see ML description in Section 2.3.3). The corresponding annual degradation cost is calculated as:

where is the battery’s Ah rating and (\$/kWh) is the battery capital cost.

The total annual cost is then estimated based on the calculated operations cost, battery depreciation and degradation cost, and depreciation cost for other equipment such as balance of plant.

(11)

The annual net revenues from the hydro hybrid system are then calculated using the total revenue and total annual cost as:

Table 4. Techno-economic parameters used for financial performance evaluation. Note that the scenarios are drawn from [41].

Scenarios							Units
2018- low	2018- mid	2018- high	2025- low	2025- mid	2025- high		
223	271	323	156	189	203	\$/kWh	
230	288	470	184	211	329	\$/kW	
80	100	120	75	95	115	\$/kW	
92	101	110	87	96	105	\$/kWh	
		10				\$/kW-yr	
		5				%	
		1.79				%	
		25				%	
		10				years	
		10				years	

2.4.2. Financial performance metrics

The financial performance metrics evaluated in this study are:

- Return on investment (ROI) – Measure of the percentage of returns generated by an investment (or project) relative to its total investment [42]. ROI estimates the future benefits generated by a project and divides those benefits by the total investment. In this paper, ROI is used to compare

the performance of different battery configurations over 5 years () and is calculated as:

- Payback period – The time to break-even, i.e., when cash generated by the project pay off the investment costs. The payback period in years is calculated by dividing total initial investment by the annual cash flow, without considering the time value of money.
- Net present value (NPV) – Difference between current value of cash inflows and cash outflows over a certain period of time, taking into account the time value of money. Positive NPVs are favorable, as they indicate that future cash generation exceeds initial and ongoing cash expenses. NPV is calculated as [43]:
- Internal rate of return (IRR) – The discount rate at which the NPV of all cash flows (both positive and negative) of a project or investment equals zero. Positive IRRs and new-project IRRs that exceed the required rate of return or discount rate are desirable. IRR is used to evaluate the attractiveness of a project based on estimated cash used and generated from the project over given time periods [44]. Mathematically, it is obtained by solving for r in (14) when $r = 0$.

These financial metrics—ROI, NPV, IRR, and payback period—are often considered in combination to evaluate projects [43, 45]. The precise set and relative weight given to each is circumstantial and varies between organizations. For instance, ROI has been used as the optimization objective to maximize the benefit of a grid-connected hybrid electrical energy storage system [46]. In other cases, NPV and IRR are used as indicators to evaluate the investment profitability and to guide capacity sizing and plant operations for hydropower plant and hydro hybrid system [47, 48]. In the present work all financial performance metrics are presented equally.

3. Results and discussions

3.1. Prediction model validation

3.1.1. Revenue Prediction

The full revenue prediction results are presented in our previous work [40]. The percent errors of annual revenue predictions and RMSE for predicted annual revenue vary from -11% to 8% and \$26.8 to \$2577.8, respectively [40]. Herein we use results from Run #17 (Site C: plant capacity = 13.4 MW with a capacity factor = 0.52; with a battery of 3.2 MW and 1.6 MWh) as an example to demonstrate the revenue predictions. Visually, revenue predicted for each day using the ML model compares well to observed values (Figure 5). The maximum daily prediction error is -29.6%, which occurred only twice (Figure 6a). Out of a total of 365 days, there are 312 days (86%) with prediction errors less than $\pm 5\%$ and 343 days (94%) with prediction errors less than $\pm 10\%$ (Figure 6b). While this could be considered a large maximum daily error, the model is primarily aggregated to annual values and because these large errors are rare, the overall annual accuracy is quite good [40].

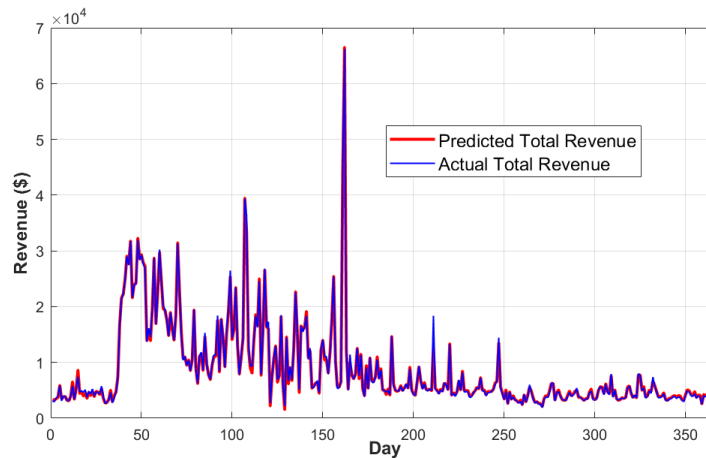


Figure 5. Comparison between actual and predicted daily revenues from Run # 17.

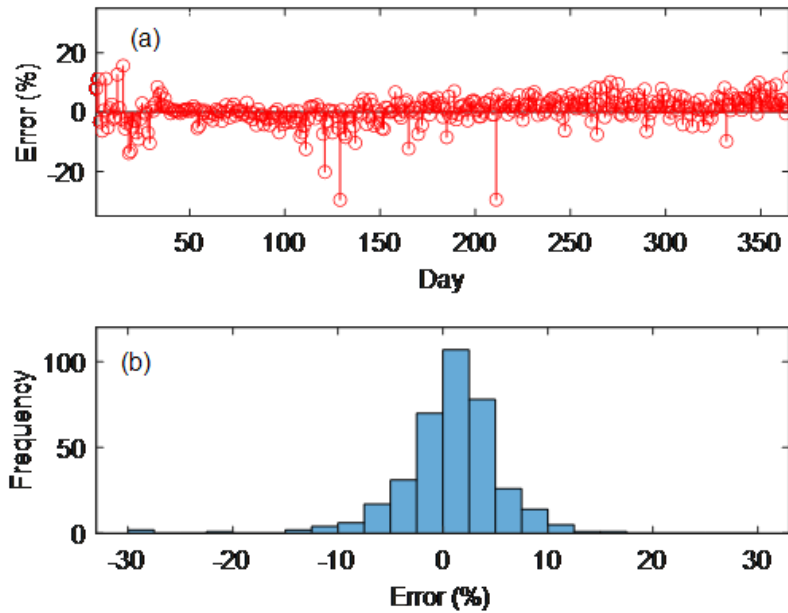


Figure 6. (a) Percent errors of daily revenue predictions and (b) histogram of the percent errors in (a) from Run # 17.

The revenue of hydro hybrids comes from both energy and ancillary markets, which include a variety of services (Figure 7), therefore the revenue streams can be categorized by service provision. These revenue streams ranked in a descending order are hydroelectricity sold directly to energy market (“Hydro Energy to Grid”), battery providing regulation up (“Storage RegUp”), battery providing electricity to energy market (“Storage Energy to Grid”), battery providing regulation down (“Storage RegDn”), and battery providing spinning reserve (“Storage Spin”). The two greatest sources of battery value are (1) being able to participate in frequency regulation and (2) energy shifting (Table 5). Depending on the particular day or market condition, the relative value of these revenue sources is likely to change (for example, see Figure 7). Even though energy generation is similar across three consecutive days in June, market prices differ considerably, resulting in very different battery operations. In essence, this highlights that the overall value of the battery is to increase flexibility, which can be used to increase revenue of produce other benefits depending on the relative market value on a given day.

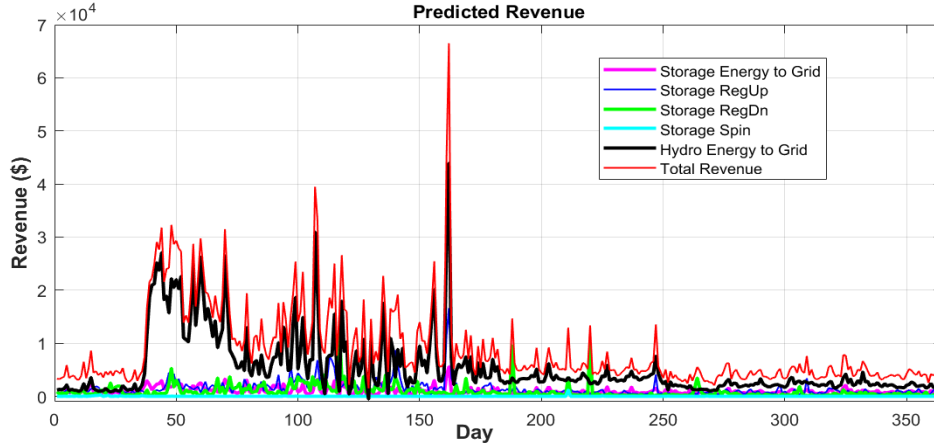


Figure 7. Example of predicted revenue by service for each day in 2019 at Site C with a battery of 3.2 MW and 1.6 MWh.

Table 5. Analysis of predicted revenue for the year 2019 at Site C with a battery of 3.2 MW and 1.6 MWh.

Statistic	Storage (Energy)	Storage (RegUp)	Storage (RegDn)	Storage (Spin)	Hydropower (Energy)
Annual Total (\$)	375,400	514,300	334,700	4,800	1,966,400
Daily Average (\$)	1,028	1,409	917	13	5,387
Daily Maximum (\$)	5,578	16,640	12,628	1,185	43,903
Standard Deviation of Daily Revenue (\$)	676	1,489	1,255	67	5,991

3.1.2. Battery degradation prediction

In this section, two evaluation metrics (percent error and RMSE) are computed to evaluate the accuracy of the trained ML model (Table 6) for the low, medium, and high degradation scenarios. The percent errors vary from -6% to 33%, -8% to 52%, and -12% to 59% in the low, medium, and high degradation scenarios, respectively (Table 6). Larger percent errors are observed for the runs with energy ratings smaller than 0.6 MWh (in Run #1 to #6) across all degradation scenarios.

Accurate battery degradation prediction emerges as a cornerstone in advancing the efficacy and longevity of lithium-ion batteries, particularly evident from the insights gleaned from previous studies. There are important things to consider when predicting battery degradation, including an in-depth understanding of battery degradation dynamics, adept feature selection, and the proficient application of ML methods. The paramount importance of feature selection cannot be overstated [49], as it steers the ML model towards pertinent aspects of the data that are most informative about the target prediction, in

this case, battery degradation. Notably, certain features like cycling time, voltage range, current rate, state of charge (SOC), temperature, depth of discharge (DOD), and energy storage time have been underscored as especially influential in predicting degradation, given their intricate link with the underlying physical and chemical processes that drive battery wear and tear [49, 50].

One of the challenges and key roadblocks in our research is that we only have price and energy generation profiles as the inputs to the ML model for predicting battery degradation, an approach that hasn't been paralleled in existing research and therefore lacks comparative analysis. Moving forward, we will explore new methodologies to refine our ML model prediction accuracy. This could potentially involve integrating additional features, testing with different ML algorithms, and possibly exploring hybrid models that might intertwine price profiles with other pertinent variables.

Although our degradation predictions present greater percent errors than the revenue predictions, the impact on the degradation costs calculation is limited since the maximum prediction error is approximately 6% in absolute terms. Note that the unit of battery degradation is also in percentage terms. For example, Run #2 in the high degradation scenario has the highest percent error of 59%, which translates to 6% in absolute terms (predicted annual capacity fade of 16% vs. actual value of 10%).

Table 6. Battery degradation prediction errors of the 18 out-of-sample test runs. Note that percent errors measure annual prediction errors, and RMSEs measure daily prediction errors.

Run #	Low degradation rate				Medium degradation rate				High degradation rate			
	Actual annual capacity fade (%)	Predicted annual capacity fade (%)	Percent error (%)	RMSE (%)	Actual annual capacity fade (%)	Predicted annual capacity fade (%)	Percent error (%)	RMSE (%)	Actual annual capacity fade (%)	Predicted annual capacity fade (%)	Percent error (%)	RMSE (%)
1	2.84	3.03	6	0.181	7.64	8.34	9	0.664	15.32	16.99	11	1.440
2	2.14	2.84	33	0.256	5.05	7.67	52	0.958	9.71	15.46	59	2.070
3	2.81	3.01	7	0.157	7.50	8.29	11	0.581	15.02	16.90	12	1.270
4	2.35	2.91	24	0.255	5.84	7.98	37	0.972	11.43	16.32	43	2.190
5	2.95	3.00	2	0.129	7.98	8.26	4	0.457	16.03	16.84	5	0.962
6	2.66	2.96	11	0.208	6.94	7.95	15	0.796	13.79	16.41	19	1.780
13	3.08	3.02	-2	0.059	8.51	8.41	-1	0.224	17.20	17.19	0	0.544
14	2.45	2.57	5	0.099	6.18	6.71	9	0.370	12.17	12.96	6	0.897
15	2.95	2.94	0	0.058	8.02	7.92	-1	0.203	16.14	16.37	1	0.519
16	2.85	2.68	-6	0.091	7.64	7.01	-8	0.354	15.33	13.74	-10	0.823
17	2.94	2.96	1	0.057	7.91	7.89	0	0.214	15.88	16.59	4	0.540
18	2.98	2.84	-5	0.075	8.09	7.62	-6	0.291	16.28	14.27	-12	0.796
31	3.08	3.09	0	0.066	8.50	8.52	0	0.210	17.20	17.23	0	0.540
32	2.94	3.00	2	0.077	7.99	8.09	1	0.268	16.08	16.45	2	0.591
33	2.95	2.98	1	0.071	8.01	8.09	1	0.249	16.12	16.37	2	0.572
34	2.96	2.94	-1	0.071	8.06	8.09	0	0.248	16.23	16.21	0	0.567
35	2.93	2.98	2	0.079	7.89	7.93	1	0.283	15.83	16.43	4	0.647
36	2.94	2.99	2	0.076	7.92	8.23	4	0.283	15.91	16.67	5	0.614

3.2. Financial evaluation of hybrid hydro systems

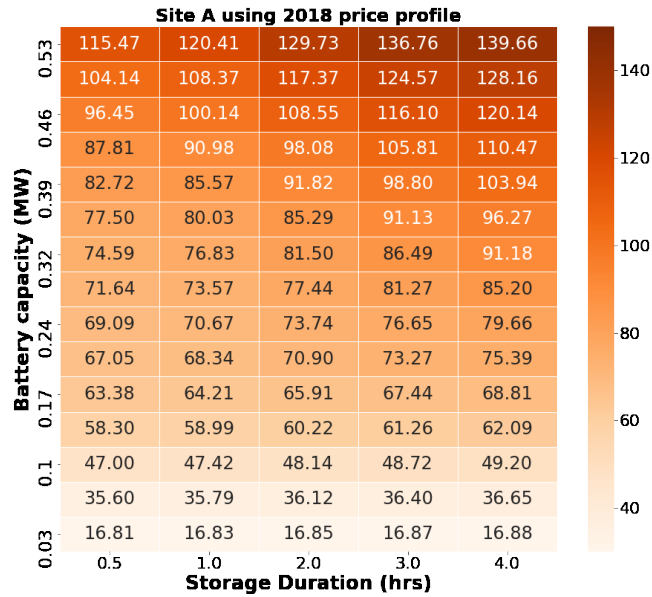
While the above results examine the prediction accuracy of revenue and battery degradation, the aim of this developed tool is to efficiently assess financial benefits. This section presents the financial performance of hybrid hydro and battery systems by applying the ML-based tool to Site A, C, and F, which represent low, medium, and high CF, respectively. Because power ratings of batteries in the 18 test cases only include the 20th and 80th percentiles of their paired hydropower plants' power duration curves, to show a refined view of the financial performance as a function of a battery's power rating, we examine 15 power ratings that are evenly distributed between the 20th and 80th percentiles of the paired power plant's power duration curve. Specifically, battery power ratings vary from 0.03 to 0.53 MW for Site A, 3.22 to 7.91 MW for Site C, and 0.96 to 1.70 MW for Site F. For each power rating, the evaluated storage durations are 0.5, 1, 2, 3, and 4 hours. We therefore examine a total of 75 battery configurations at each site.

3.2.1. Revenue increase by adding batteries

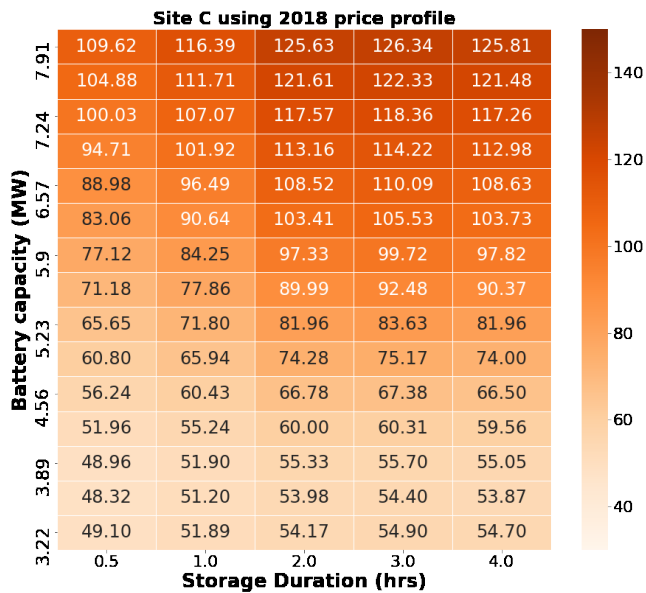
Figure 8 shows net revenue increase (%) incurred by pairing a battery to a standalone hydropower plant. The trends are consistent with expectations that increasing battery size results in larger marginal increase in revenue for small batteries and then plateaus for large batteries. As mentioned in Section 3.1.1, the revenue prediction accuracy is approximately 5%, and therefore, differences in predicted revenue less than this error are within the uncertainty bound.

We also observed that the net revenue increases vary by site (Figure 8). The net revenue increases range from 17% to 150% in Site A, as opposed to 48% to 126% and 52% to 101% in Site C and F, respectively. Besides the different ranges, the rate of revenue increases by increasing battery size also differ by site. For example, when Site A is paired with a 0.5-hour battery, the net revenue increases by about 109% when the battery's power capacity increases from 0.03 MW to 0.07 MW (133% increase), as opposed to a change of 10% when the power capacity increases from 0.49 MW to 0.53 MW (8% increase). At Site C, increasing the power capacity from 3.22 MW to 3.56 or even 3.89 MW does not lead

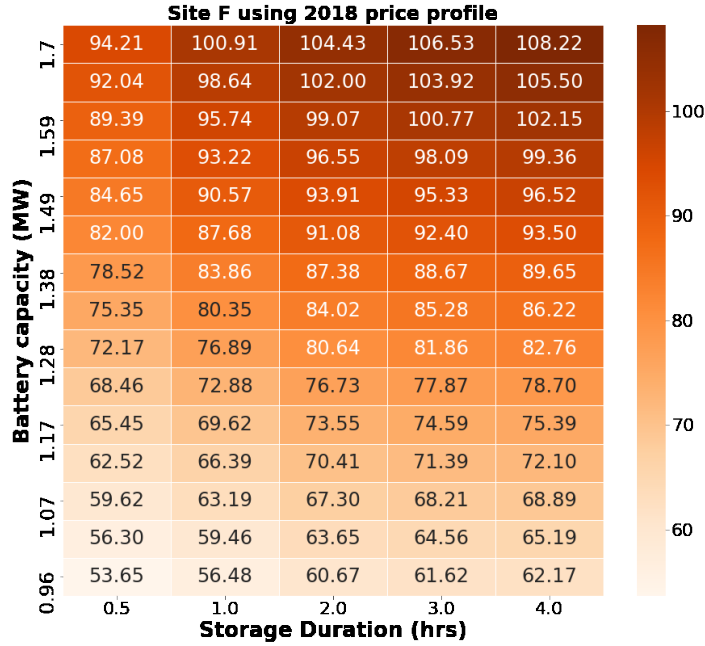
to any increase in net income. While at Site F, the percentage increase in battery power capacity leads to almost the same percentage increase in net revenue. Note that the significantly greater marginal revenue increases in Site A only occur to batteries with small power capacities, implying greater financial benefits for a small battery to increase its capacity.



(a)



(b)



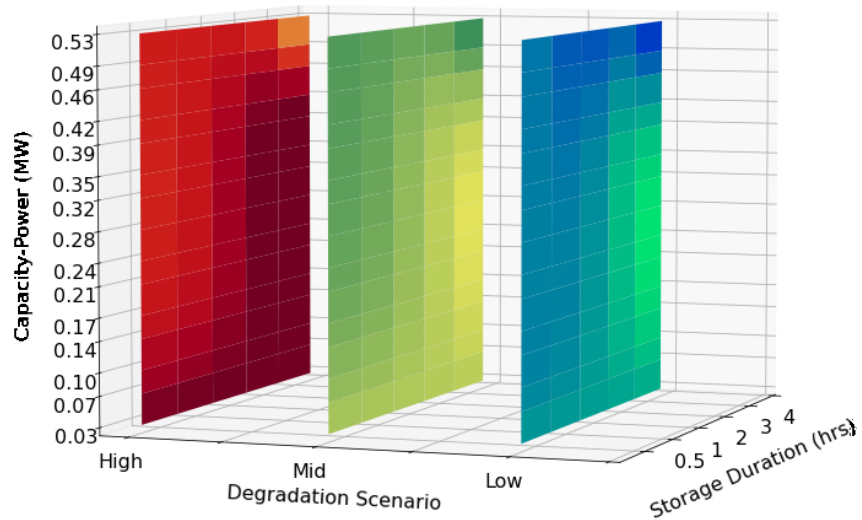
(c)

Figure 8. Revenue increase (%) by adding energy storage to a standalone hydropower plant. Numbers in cells represent percent change of revenues compared with a standalone hydropower plant. (a) Site A using 2018 price profile; (b) Site C using 2018 price profile; (c) Site F using 2018 price profile.

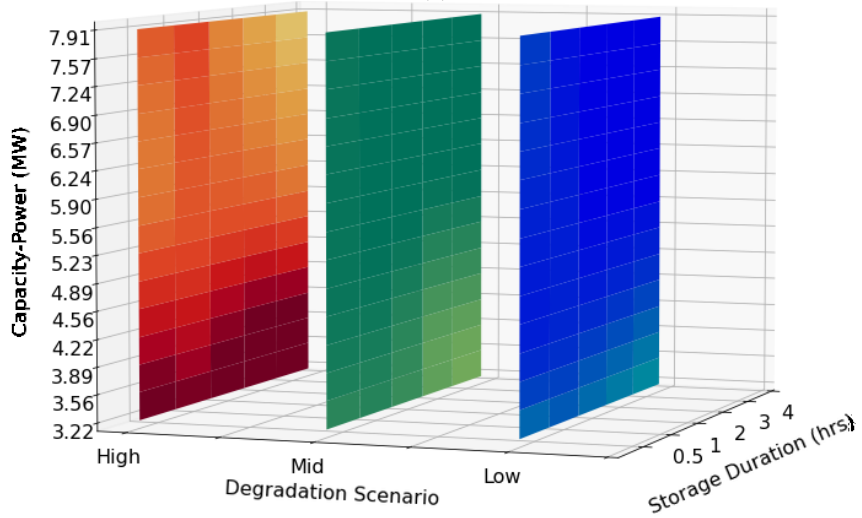
3.2.2. Battery degradation predictions across range of batteries

The ML-based battery degradation prediction model is applied under different hypothetical degradation rate scenarios (i.e., low, medium, and high as described in Section 2.2). For Site A, the predicted annual battery capacity fades range from 2.84% to 3.09%, 7.67% to 8.47%, and 15.46% to 17.24% for the low, medium, and high degradation scenarios, respectively. For Site C, the predicted annual battery capacity fades range from 2.51% to 2.99%, 6.59% to 8.38%, and 13.02% to 17.19% under the low, medium, and high degradation scenarios, respectively. For Site F, the predicted annual battery capacity fades range from 2.98% to 3.12%, 8.00% to 8.62%, and 16.42% to 17.56% for the low, medium, and high degradation scenarios, respectively. When storage duration is kept constant, increasing power capacity tends to reduce capacity fade slightly (Figure 9). These trends are consistent with the results of physics-based model in Table 2, implying that the ML-based model can capture the effects of battery

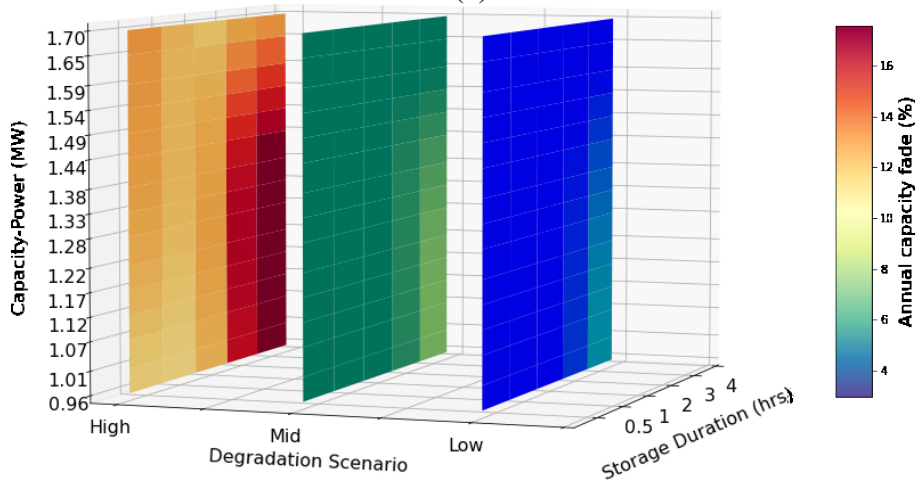
sizes on degradation.



(a)



(b)



(c)

Figure 9. Predicted annual capacity fades (%) of batteries as a function of power capacity and storage duration for (a) Site A, (b) Site C and (c) Site F using the 2018 price profile.

3.2.3. Financial performance optimization

The financial metrics of the low degradation scenario are presented in Figure 10. Considering battery degradation, the 5-year cumulative ROI ranges from 38.56% to 485.42%, 41.11% to 238.51%, and 57.06% to 238.97% in Site A, C, and F, respectively (Figure 10). The optimal battery sizes are found to be 0.03 MW and 0.015 MWh at Site A, 3.22 MW and 1.61 MWh at Site C, and 1.44 MW and 0.72 MWh at Site F. All of the optimal capacities are at the bottom left corner as a result of the associated low capital and operations costs. In addition, the tool also shows different impacts of battery capacities on ROIs across sites. For instance, at Site A (plant capacity = 3.1 MW), the maximum 5-year cumulative ROI is about 10 times higher than the minimal, whereas at Site C (plant capacity = 13.4 MW) and Site F (plant capacity = 2.2 MW), the maximum ROI is about 4 to 5 times higher than the minimal. This result suggests that financial performance of hydro hybrid systems can be largely influenced by site-specific characteristics, such as energy generation profiles, which directly impact revenue from various energy and ancillary services markets. The price profile also significantly shapes the revenue, aligning the energy supplied to each market with concurrent market prices. Thus, it becomes imperative to conduct an independent evaluation of the financial benefits for each individual case, considering the intricate relationship between energy generation and market prices to accurately gauge and optimize the potential financial gains. At Site F, ROIs of batteries with the same storage duration span a very narrow range (relative standard deviations for each storage duration range from 0.80% to 1.39%), suggesting greater sensitivity to storage duration than to power rating at this site. At Site F, the high capacity factor (CF = 0.81) suggests steady energy output, leading to more stable and predictable revenue than other two sites, which in turn results in a less fluctuating ROI. Given this consistent energy production, any extra revenue from introducing a battery, particularly one with a larger capacity, can be lower. However, extending storage durations can enable the plant to capitalize on energy sales during peak times by storing energy in low-demand periods, offering a higher revenue boost than enhancing battery capacity.

The payback period ranges from 0.97 to 6.32 years in Site A, 1.88 to 6.13 years in Site C, and 1.91 to 5.16 years in Site F (Figure 10). Similar to the ROIs, the impact of battery sizes on payback period varies

by site. For example, when a 4-hour battery is paired with Site A, a power rating of 0.53 MW results in a 50% longer payback period than a power rating of 0.03 MW. By contrast, for Site C and F, batteries with the same storage duration but different power ratings yield similar payback periods. This result implies that the marginal benefit of adding a battery with a different power rating is minimal, resulting in nearly equivalent added revenues and costs. This leads to similar payback periods for batteries of varying power ratings but consistent storage durations. On the other hand, increasing the storage duration in these two sites allows for enhanced revenue generation by optimizing energy storage during low demand and selling during peak periods, outweighing the associated costs.

Following assumptions in [41], we assume a discount rate of 1.79% to account for the time value of money in the NPV calculation. The resulting NPVs vary from \$0.09 million to \$0.65 million, \$2.95 million to \$12.58 million, and \$1.19 million to \$3.01 million in Site A, C, and F, respectively (Figure 10). Unlike the ROI and payback period results, where smaller battery sizes are preferred, the highest NPVs are usually associated with the greatest power ratings due to greater annual revenues. Note that NPV measures the investment by discounting all cash flows over the project life into present values, while ROI and payback period measure the efficiency of the investment by calculating the ratio between upfront investment and annual revenue. A higher NPV therefore only indicates higher net revenues over the project life but does not necessarily mean a more efficient investment. Therefore, NPV is an appropriate optimization objective if an investor is more interested in future net assets; otherwise, metrics like ROI and payback period are more helpful to determine the optimal sizes.

The IRR is calculated to determine a discount rate at which a project breaks even (i.e., its NPV equals zero). Similar to ROI and payback period, IRR is commonly used to analyze the return on investment; however, IRR focuses more on the annual growth rate rather than the overall growth over the investment period. Thus, although the IRR plots show the same optimal sizes and trends as the ROI and payback period plots, there are still differences across these plots. For example, at Site A, a 0.5-hour battery rated at 0.46 MW has an ROI of 163.39%, which is 3% lower than a battery rated at 0.49 MW. By contrast, both configurations result in the same IRR of 37%.

In this section, the predicted 5-year cumulative ROI, payback period, IRR and NPV are presented to determine the optimal battery sizes that lead to the strongest financial performance for three selected sites. The identified optimal sizes and trends are highly site-specific. In this study, smaller power ratings and shorter storage durations can yield better financial performance in terms of ROI, payback period and IRR, whereas greater NPVs are usually associated with larger power ratings and 0.5-hr storage duration due to their higher annual revenues. Different from the ROI and payback period figures, which only indicate one single optimal sizing, the IRR figures give multiple optimal sizes that provide same annual return rates. We conclude that the developed sizing optimization tool can provide financial performance analysis and information to help decision-makers to consider the investment from different financial perspectives.

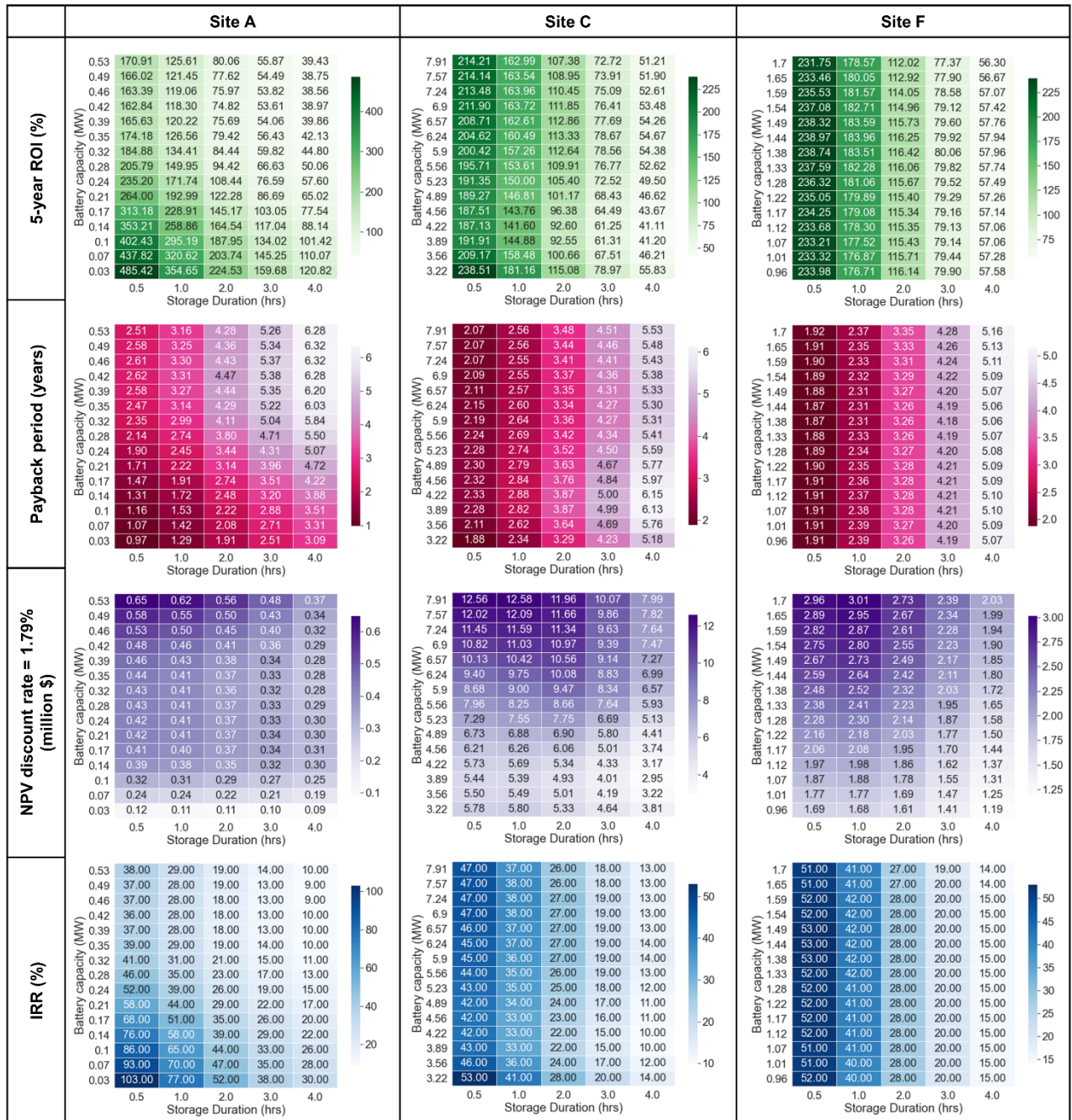
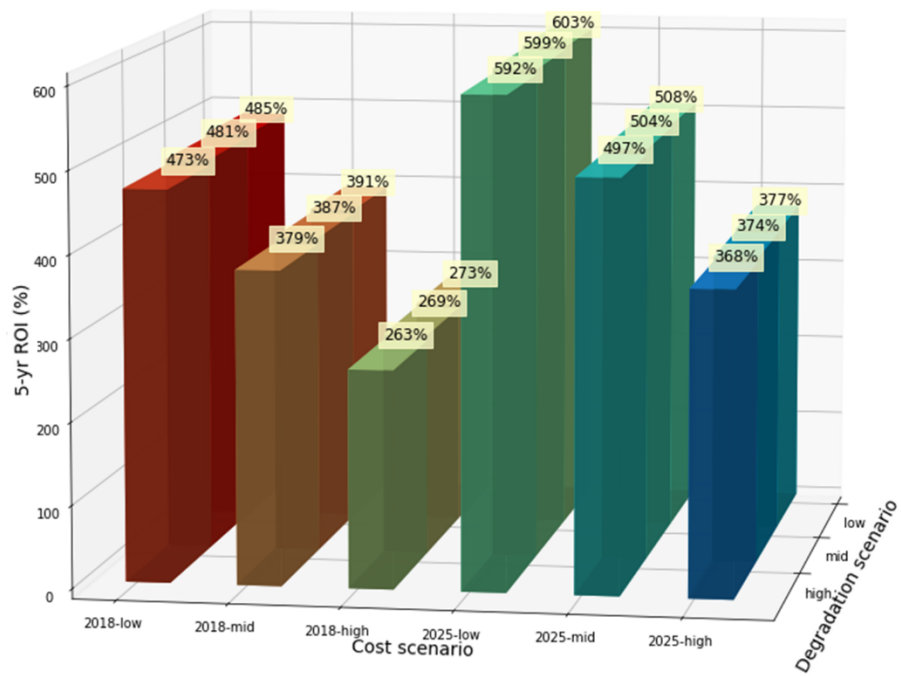


Figure 10. Financial performances of hydro hybrids at Site A, C, and F based on revenue prediction and cost estimation (using 2018 price profile). Metrics include 5-year ROI (%), payback period (years), NPV_with discount rate = 1.79% (million \$), and IRR (%). Darker colors indicate better financial performance. Note that only the low battery degradation scenario is presented.

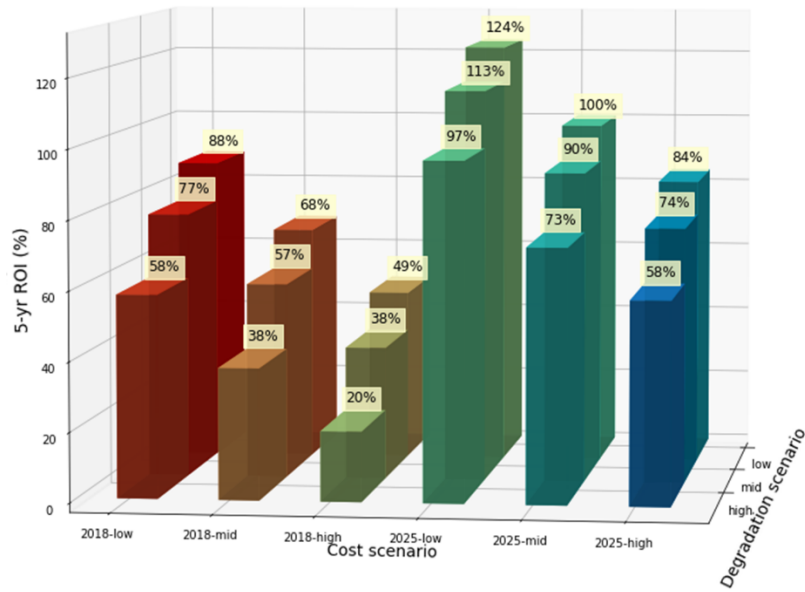
3.2.4. Impacts of battery degradation cost and cost parameters on financial performances

Including battery degradation cost can impact the estimated overall technical and financial performance of the hybrid hydro system by adding annual investment to compensate the capacity. We calculate the 5-year cumulative ROIs under three battery degradation scenarios (Table 2) and six cost scenarios (Table 4) and compare three battery configurations: optimal configuration that yields the highest ROI (Figure 11a), a median configuration that yields a medium ROI (Figure 11b), and the worst configuration that has the lowest 5-year cumulative ROI (Figure 11c).

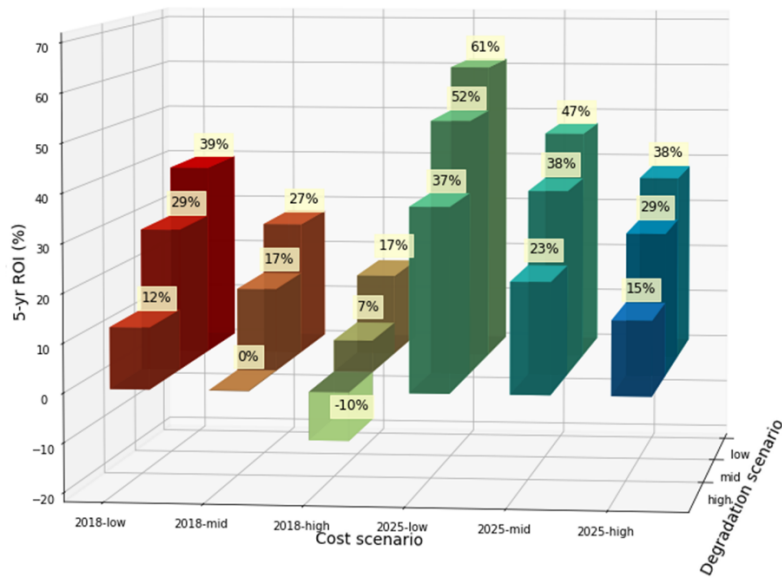
The results show that a declining battery cost results in greater financial benefits from adding energy storage. In addition, the optimal battery configuration leads to not only the highest investment efficiency but also the lowest sensitivity of financial performance to battery degradation and cost scenarios. For instance, at Site A, in the 2018-high cost scenario, if the optimal configuration is chosen, the ROI in the high degradation scenario (ROI = 263%) decreases by 4% compared the low degradation scenario (ROI= 273%) (Figure 11a); in contrast, if the worst configuration is chosen, the high degradation scenario (ROI = -10%) would result in a 270% ROI decrease compared to the low degradation scenario (ROI = 17%) (Figure 11c). The trend is also observed in other evaluated financial performance metrics at Site C and Site F (Figure S-1 and S-2). Similarly, if battery cost increases, for example, switching from the 2018-low cost scenario to the 2018-high cost scenario, the ROI decreases by 44% when using the optimal configuration across different degradation scenarios (Figure 11a), as opposed to 44-89% and 56-183% when the medium (Figure 11b) and worst configurations are used (Figure 11c).



(a)



(b)



(c)

Figure 11. 5-year ROI (%) for Site A based on revenue predictions and cost estimations under different battery cost and degradation scenarios. (a) Battery capacity = 0.03 MW, storage duration = 0.5 hrs (the configuration associated with the highest ROI); (b) battery capacity = 0.53 MW, storage duration = 4.0 hrs (the configuration associated with medium ROI); (c) battery capacity = 0.14 MW, storage duration = 4.0 hrs (the configuration generates the lowest ROI).

3.3. Limitations and future work

This generation and battery sizing tool makes significant progress in representing financial performance of this class of hybrids and helping industry take the first step in determining whether hybridization may provide a strong value proposition to them. Follow-on work is needed, though, to help represent the diversity of real-world decision-making criteria for hybridization. For example, interconnection agreements limit the maximum amount of energy that a co-located hybrid can supply to the grid at any one time. Modifications to this tool could be made to constrain use of the energy storage so that it limits the peak and instead increases the duration when the hybrid plant is providing this maximum power output to the grid. Additionally, this tool assumes perfect foresight based on participation in the real-time market. For some types of generation, such as hydropower, geothermal, and nuclear, this is a reasonable assumption. Yet, for wind and solar, generation forecast uncertainty is more important and would limit the revenue potential.

Another limitation of the model is that it is currently limited to modeling ROR hydropower plants. This could be extended in future work by training the algorithm on data from solar or wind plant studies to develop other, generation specific tools. The performance will be generation specific because differences in dispatchability, predictability, and variability drive different operating modes for the energy storage device and subsequently different revenues. For example, adding batteries has been shown to increase revenues for wind plants by 18% by reducing the imbalance cost in real-time markets [51]. This would not be captured in the current tool because ROR hydropower is much easier to predict than wind and solar, so the value of increased predictability is not well captured in the training data.

This analysis suggests that battery degradation plays an important role in the financial performance of the entire hybrid generation and battery system. The battery degradation model used in this analysis only represents a specific type of lithium-ion battery. Real-world battery degradation performance can vary substantially depend on the degradation parameters, as shown in Eq. (1). Future work should conduct sensitivity analysis to characterize the effects of other battery degradation parameters on the financial performance. In addition, we will explore optimization strategies that prioritize maximizing revenue while

also strategically minimizing battery cycles and degradation loss, through measures such as constraining the maximum and minimum SOC and limiting the number of charge/discharge cycles. Future work can incorporate degradation costs into the optimization model by representing them as additional constraints or penalty functions in the objective function. The insights drawn from this analysis can better inform stakeholders of the most appropriate battery sizes and help operators to determine the optimal operating strategies to extend battery life when coupled to renewable resources.

Future work could also explore how additional energy storage technologies paired with generation would perform financially. One example is a hybrid energy storage system composed of a Lithium-ion battery and ultracapacitor [52-54], which could potentially enhance the financial performance through using the Lithium-ion battery for services such as energy shifting, which occur a few times per day, and the ultracapacitor for frequency regulation, which includes many small charge and discharge cycles. Other energy storage technologies, such as flow batteries, iron air batteries or hydrogen paired with generation could also be considered [55, 56].

4. Conclusions

Flexibility is becoming more valuable, a trend that is expected to continue in part due to ambitious wind and solar photovoltaic generation deployment. Hybridization with batteries or other forms of energy storage is one potential way for generation to contribute more to evolving grid needs and increase revenue. Accelerating the adoption of hybridization requires providing industry with easy-to-use and open-source tools for sizing an energy storage system investment to be paired with their generation assets. This work advances that objective by developing a ML-based sizing tool that estimates financial performance of different battery sizes as part of a hybridization project.

The optimal battery sizing is heavily determined by the site-specific energy generation and plant's capacity factor, as these elements directly influence the incremental revenue achieved through battery integration and subsequently determine the financial performance of the hybrid system, especially when factoring in battery capital, operating and degradation costs. In general, batteries with smaller power

ratings and shorter storage durations can yield higher investment efficiency in terms of ROI, payback period and IRR. When battery prices continue to fall, the investment potential will become even stronger. In addition, the results suggested that choosing the optimal size not only leads to the best financial performance, but also reduces the sensitivity of financial performance to changes in cost parameters, such as higher degradation costs or capital investment costs.

In future, the team is committed to further enhancing the capabilities of the tool by adapting it to additional U.S. electricity markets beyond CAISO, while also refining the important parameters related to battery wear and tear. Future efforts will also likely explore various pairings of generation and storage technologies, such as combining lithium-ion batteries and/or ultracapacitors, to further optimize investment value. The overarching aim of this work is to aid industry leaders in adapting to the fast-evolving landscape of storage technologies and market dynamics. This guidance is intended to bolster industry investments that enhance the reliability and resilience of the power system.

Acknowledgements

This work is authored by Idaho National Laboratory, operated by Battelle Energy Alliance, LLC, under DOE Contract No. DE-AC07-05ID14517 and supported by the HydroWIREs Initiative of DOE's Water Power Technologies Office.

References

- [1] W. Gorman *et al.*, "Motivations and options for deploying hybrid generator-plus-battery projects within the bulk power system," *The Electricity Journal*, vol. 33, no. 5, p. 106739, 2020.
- [2] J. H. Kim *et al.*, "Project developer options to enhance the value of solar electricity as solar and storage penetrations increase," *Applied Energy*, vol. 304, p. 117742, 2021.
- [3] A. D. Mills *et al.*, "Solar-to-Grid: Trends in System Impacts, Reliability, and Market Value in the United States with Data through 2019," Lawrence Berkeley National Lab.(LBNL), Berkeley, CA (United States), 2021.
- [4] T. R. Nudell, A. M. Annaswamy, J. Lian, K. Kalsi, and D. D'Achiardi, "Electricity markets in the United States: a brief history, current operations, and trends," in *Smart Grid Control*: Springer, 2019, pp. 3-27.
- [5] H. Zhao, Q. Wu, S. Hu, H. Xu, and C. N. Rasmussen, "Review of energy storage system for wind power integration support," *Applied energy*, vol. 137, pp. 545-553, 2015.
- [6] T. Wang, "Battery assisted conventional generator in pjm frequency regulation market," in *2019 IEEE Power & Energy Society General Meeting (PESGM)*, 2019: IEEE, pp. 1-5.
- [7] S. A. LEFTON, P. M. Besuner, and D. D. Agan, "The real cost of on/off cycling," *Modern power systems*, no. OCT, pp. 11-13, 2006.
- [8] D. Lew, G. Brinkman, N. Kumar, P. Besuner, D. Agan, and S. Lefton, "Impacts of wind and solar on emissions and wear and tear of fossil-fueled generators," in *2012 IEEE power and energy society general meeting*, 2012: IEEE, pp. 1-8.
- [9] M. C. Such and C. Hill, "Battery energy storage and wind energy integrated into the Smart Grid," in *2012 IEEE PES Innovative Smart Grid Technologies (ISGT)*, 2012: IEEE, pp. 1-4.
- [10] C. A. Hill, M. C. Such, D. Chen, J. Gonzalez, and W. M. Grady, "Battery energy storage for enabling integration of distributed solar power generation," *IEEE Transactions on smart grid*, vol. 3, no. 2, pp. 850-857, 2012.
- [11] S. Shafiu Alam *et al.*, "Idaho Falls Power Black Start Field Demonstration (Preliminary Outcomes Paper)," Idaho National Lab.(INL), Idaho Falls, ID (United States); National ..., 2021.
- [12] M. Roni *et al.*, "Hydropower flexibility valuation tool for flow requirement evaluation," *Energy Reports*, vol. 9, pp. 217-228, 2023.
- [13] J. Wang *et al.*, "Cycle-life model for graphite-LiFePO₄ cells," *J. Power Sources*, vol. 196, no. 8, pp. 3942-3948, 2011.
- [14] A. Barré, B. Deguilhem, S. Grolleau, M. Gérard, F. Suard, and D. Riu, "A review on lithium-ion battery ageing mechanisms and estimations for automotive applications," *J. Power Sources*, vol. 241, pp. 680-689, 2013.
- [15] A. Ahmadian, M. Sedghi, A. Elkamel, M. Fowler, and M. A. Golkar, "Plug-in electric vehicle batteries degradation modeling for smart grid studies: Review, assessment and conceptual framework," *Renew. Sust. Energ. Rev.*, vol. 81, pp. 2609-2624, 2018.
- [16] A. Krupp, R. Beckmann, T. Diekmann, E. Ferg, F. Schuldt, and C. Agert, "Calendar aging model for lithium-ion batteries considering the influence of cell characterization," *Journal of Energy Storage*, p. 103506, 2021.
- [17] S. Barcellona and L. Piegari, "Effect of current on cycle aging of lithium ion batteries," *Journal of Energy Storage*, vol. 29, p. 101310, 2020.
- [18] C. A. Murphy, A. Schleifer, and K. Eurek, "A taxonomy of systems that combine utility-scale renewable energy and energy storage technologies," *Renewable and Sustainable Energy Reviews*, vol. 139, p. 110711, 2021.
- [19] P. L. Denholm, R. M. Margolis, and J. D. Eichman, "Evaluating the technical and economic performance of PV plus storage power plants," Golden, CO, 2017.
- [20] M. Mahalik, T. Veselka, A. Mahajan, and F. T. Bui, "Application of a New Tool to Optimize Hydropower Day-Ahead Scheduling and Real-Time Operations," Louisville, KY, 2012.
- [21] D. Wu, C. Jin, P. Balducci, and M. Kintner-Meyer, "An energy storage assessment:

- Using optimal control strategies to capture multiple services," 2015 2015, pp. 1-5.
- [22] K. H. Anderson *et al.*, "REopt: A platform for energy system integration and optimization," Golden, CO, 2017.
- [23] N. Blair *et al.*, "System advisor model, sam 2014.1. 14: General description," Golden, CO, 2014.
- [24] W. Chen, W. Zou, K. Zhong, and A. Aliyeva, "Machine learning assessment under the development of green technology innovation: A perspective of energy transition," *Renewable Energy*, 2023.
- [25] S. T. Shabestari, A. Kasaeian, M. A. V. Rad, H. F. Fard, W.-M. Yan, and F. Pourfayaz, "Techno-financial evaluation of a hybrid renewable solution for supplying the predicted power outages by machine learning methods in rural areas," *Renewable Energy*, vol. 194, pp. 1303-1325, 2022.
- [26] T. M. Alabi *et al.*, "A review on the integrated optimization techniques and machine learning approaches for modeling, prediction, and decision making on integrated energy systems," *Renewable Energy*, vol. 194, pp. 822-849, 2022.
- [27] Z. Zhang *et al.*, "Operation rule extraction based on deep learning model with attention mechanism for wind-solar-hydro hybrid system under multiple uncertainties," *Renewable Energy*, vol. 170, pp. 92-106, 2021.
- [28] L. Wang *et al.*, "A novel cost-efficient deep learning framework for static fluid–structure interaction analysis of hydrofoil in tidal turbine morphing blade," *Renewable Energy*, vol. 208, pp. 367-384, 2023.
- [29] M. Mahalik, T. Veselka, A. Mahajan, and F. T. Bui, "Application of a New Tool to Optimize Hydropower Day-Ahead Scheduling and Real-Time Operations," in *Proceedings of HydroVision International 2012*, Louisville, KY, July 2012 2012.
- [30] R. Coughlan and W. Jian, "Lingo The Modeling Language and Optimizer," *Chicago: LINDO Systems Inc*, 2018.
- [31] USGS. "USGS Water Data for the Nation." <https://waterdata.usgs.gov/nwis> (accessed 2021).
- [32] U.S. Energy Information Administration. *Form EIA-860. U.S. Energy Information Administration*. [Online]. Available: <https://www.eia.gov/electricity/data/eia860/>
- [33] T. R. Tanim and C. D. Rahn, "Aging formula for lithium ion batteries with solid electrolyte interphase layer growth," *J. Power Sources*, vol. 294, pp. 239-247, 2015.
- [34] T. R. Tanim, C. D. Rahn, and N. Legnedahl, "Elevated temperatures can extend the life of lithium iron phosphate cells in hybrid electric vehicles," in *Dynamic Systems and Control Conference*, 2015, vol. 57250: American Society of Mechanical Engineers, p. V002T26A003.
- [35] M. Garg, T. R. Tanim, C. D. Rahn, H. Bryngelsson, and N. Legnedahl, "Elevated temperature for life extension of lithium ion power cells," *Energy*, vol. 159, pp. 716-723, 2018.
- [36] S. Grolleau *et al.*, "Calendar aging of commercial graphite/LiFePO₄ cell–Predicting capacity fade under time dependent storage conditions," *Journal of Power Sources*, vol. 255, pp. 450-458, 2014.
- [37] Y. Preger *et al.*, "Degradation of commercial lithium-ion cells as a function of chemistry and cycling conditions," *Journal of The Electrochemical Society*, vol. 167, no. 12, p. 120532, 2020.
- [38] W. Cole, A. W. Frazier, and C. Augustine, "Cost Projections for Utility-Scale Battery Storage: 2021 Update," 2021.
- [39] V. Nair and G. E. Hinton, "Rectified linear units improve restricted boltzmann machines," in *Proceedings of the 27th international conference on machine learning (ICML-10)*, 2010, pp. 807-814.
- [40] Y. Lin *et al.*, "Revenue prediction for integrated renewable energy and energy storage system using machine learning techniques," *Journal of Energy Storage*, vol. 50, p. 104123, 2022.
- [41] K. Mongird *et al.*, "Energy storage technology and cost characterization report," Richland, WA, 2019.
- [42] Caroline Banton. "Return on Investment vs. Internal Rate of Return: What's the

- Difference?" <https://www.investopedia.com/articles/investing/111715/return-investment-roi-vs-internal-rate-return-irr.asp> (accessed Dec 20, 2022).
- [43] G. Dandy, T. Daniell, B. Foley, and R. Warner, *Planning & Design of Engineering Systems*. CRC Press, 2017.
- [44] L. J. Gitman, R. Juchau, and J. Flanagan, *Principles of managerial finance*. Pearson Higher Education AU, 2015.
- [45] Y. R. Pasalli and A. B. Rehiara, "Design planning of micro-hydro power plant in hink river," *Procedia Environmental Sciences*, vol. 20, pp. 55-63, 2014.
- [46] D. Zhu, Y. Wang, S. Yue, Q. Xie, M. Pedram, and N. Chang, "Maximizing return on investment of a grid-connected hybrid electrical energy storage system," in *2013 18th Asia and South Pacific Design Automation Conference (ASP-DAC)*, 2013: IEEE, pp. 638-643.
- [47] A. Santolin, G. Cavazzini, G. Pavese, G. Ardizzon, and A. Rossetti, "Techno-economical method for the capacity sizing of a small hydropower plant," *Energy Conversion and Management*, vol. 52, no. 7, pp. 2533-2541, 2011.
- [48] F. Kose, M. N. Kaya, and M. Ozgoren, "Use of pumped hydro energy storage to complement wind energy: a case study," *Thermal Science*, vol. 24, no. 2 Part A, pp. 777-785, 2020.
- [49] K. A. Severson *et al.*, "Data-driven prediction of battery cycle life before capacity degradation," *Nature Energy*, vol. 4, no. 5, pp. 383-391, 2019.
- [50] H. Rauf, M. Khalid, and N. Arshad, "Machine learning in state of health and remaining useful life estimation: Theoretical and technological development in battery degradation modelling," *Renewable and Sustainable Energy Reviews*, vol. 156, p. 111903, 2022.
- [51] M. Dadashi, K. Zare, H. Seyedi, and M. Shafie-khah, "Coordination of wind power producers with an energy storage system for the optimal participation in wholesale electricity markets," *International Journal of Electrical Power & Energy Systems*, vol. 136, p. 107672, 2022.
- [52] A. Banerjee, T. M. Mosier, and S. Shafiul Alam, "Impact of Hybrid Energy Storage System (HESS) Topologies on Performance: Exploration for Hydropower Hybrids," Idaho National Lab.(INL), Idaho Falls, ID (United States), 2021.
- [53] Y. Kim, V. Raghunathan, and A. Raghunathan, "Design and management of hybrid electrical energy storage systems for regulation services," in *International Green Computing Conference*, 2014: IEEE, pp. 1-9.
- [54] V. K. Singh, Y. Lin, B. Li, R. Bhattarai, and T. M. Mosier, "A Technoeconomic Assessment Methodology of Energy Storage Systems for Dynamic Frequency Regulation," in *2022 IEEE Power & Energy Society General Meeting (PESGM)*, 2022: IEEE, pp. 1-5.
- [55] S. Wang *et al.*, "Analyses and optimization of electrolyte concentration on the electrochemical performance of iron-chromium flow battery," *Applied Energy*, vol. 271, p. 115252, 2020.
- [56] F. Díaz-González, A. Sumper, O. Gomis-Bellmunt, and F. D. Bianchi, "Energy management of flywheel-based energy storage device for wind power smoothing," *Applied energy*, vol. 110, pp. 207-219, 2013.